Chapter 1

Two-Phase Inverters with Minimum Switching Devices

Branislav Dobrucky, Tomas Laskody and
Roman Konarik

Additional information is available at the end of the chapter

http://dx.doi.org/10.5772/67743

Abstract

The chapter deals with two-phase inverters with minimum switching devices whereby the main emphasis is devoted to 'minimum switches' converter topologies and control of passive load as well as split-single-phase induction motor. Such a converter consists of one-leg half-bridge matrix converter and the ac neutral point network as a new type of converter with two phase outputs loading the resistive-inductive or motoric loads. As harmonic content of the voltage of both phases gives very high value of total harmonic distortion (THD), roughly 86%, the current waveforms should be improved by using serial LC filter that brings much more suitable value of THD. Besides, the running capacitor creating needed phase shift (90°) is electronically switched due to varied load. Analysis and modeling of such a new type of single-leg ac/ac converter with two phase outputs are done. The proposed topologies were simulated by Matlab/Simulink and verified in an LT spice environment. Worked-out simulation results are in good agreement with theoretical assumptions and make possible to give recommendation for the fair and right design of the chosen type of converter. Combination of mentioned measures brings a good quality of output quantities of converter and represents the main contribution of the chapter.

Keywords: two-phase inverter, matrix converter, one-leg VSI converter, LC resonant filter, half bridge connection, bidirectional switch, modeling, LT Spice simulation

1. Introduction

In spite that the generation and transmission of electric power are done by means of the three-phase ac system, today, the development of the two-phase system is still continued mainly to split-single-phase IM motor supply that is documented in this chapter and given references. So, the first venture into the realm of polyphase electric power has used only two alternating

current phases rather than three but with pulsating power flow to motor in contrast to constant power of three-phase system [1]. In regard to topologies of the two-phase inverters, mostly three-leg ones with six switches or two legs with four switches are used. Evaluation of low-cost topologies for the two-phase induction motor (IM), which drives in an industrial application, is analyzed and discussed in Refs. [2–4]. Half-bridge two-phase voltage source inverters (VSI) for two-phase (IM) supply are described in Refs. [5–8]. Besides, there exists also a possibility to supply three-phase induction motor by the two-phase inverter [9].

Regarding to minimum switching devices, two-phase one-leg VSI inverters for the two-phase IM supply, there are works of Chomat et al. in Refs. [10–12]. In those, the operation of the motor at nominal frequency is different from the reduced frequency operation when phase shift of auxiliary phase is provided by a capacitor. Due to variable load, it is useful to change the value of capacitance in auxiliary phase, so the electronically switched capacitor techniques are used [13, 14]. Current pulse-width-modulation (PWM) or space vector modulation (SWM) provides demanded sinusoidal waveform and feedback control [15, 16].

A new original topology of single-leg direct matrix converter was first published by authors of this chapter in Ref. [17] based on the works in Refs. [10, 18]. The number of switches is minimized, but total harmonic distortion (THD) of auxiliary-phase voltage is very high (86% at 50 Hz, 69% at 33.33 Hz) and consequently current distortions too (68 and 43%, respectively). Therefore, the improved two-phase one-leg matrix converter is completed by an LC filter [19] designed by Dobrucký et al. [20]. Combination of tuned LC filter and switched capacitor brings a new quality of output quantities of converter, which provides acceptable THD and makes possible field-oriented control (FOC) of the IM motor.

The chapter is organized as follows. First, the basic topologies of one-, two-, three-, and four-leg VSI inverters for two-phase application are described. Next, the special topologies using matrix inverters for two-phase application are introduced. Possibilities of use of switched capacitor for auxiliary circuit phase control providing the use of LC filter are described, and simulation study of Matlab/Simulink and LT Spice with passive RL and active motoric loads are given. Afterward, current controlled PWM (or hysteresis control) is worked out, and finally, conclusion is described.

2. Basic topologies of VSI inverters for two-phase application

2.1. Two-phase voltage source inverter with two legs

The topology (**Figure 1**) consists of four semiconductor switches. A low number of a semiconductor switches is the main advantage of the topology. Those switches create two half-bridge inverters, each of them powers one of the windings. The disadvantage, which this topology suffers from, is low magnitude of the output voltage. It is half of an interlink DC voltage in Refs. [2, 21]. Another disadvantage is hidden in control of the switches, which is only bipolar PWM can be used [6], which has further negative consequences.

It is also possible to supply three-phase IM motor by two-phase VSI inverter [9], **Figure 2**.

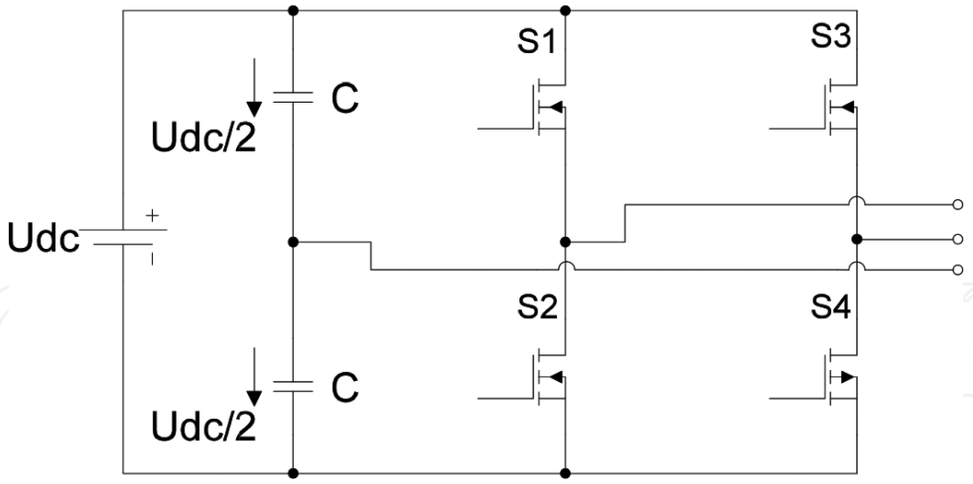

Figure 1. Voltage source inverter with two legs.

In opposite, there is also a possibility to supply two-phase IM by three-phase three-leg inverter (at the next).

2.2. Two-phase voltage source inverter with three legs

The topology shown in **Figure 3** consists of six semiconductor switches. Two of the three-leg are used for the power supply of the motor windings and third leg is used for creation of common phase of the motor [2, 21]. As a control of the switches, the modified SPWM [6, 22] can be used to describe the use of sin(ωt), cos(ωt), and –sin(ωt) as the reference voltages. The advantage compared to the converter with two legs is in better usage of a DC interlink. While inverter with two legs can put only half of DC voltage interlink magnitude, inverter with three legs is able to use $U_{\mathrm{DC}}/\sqrt{2}$.

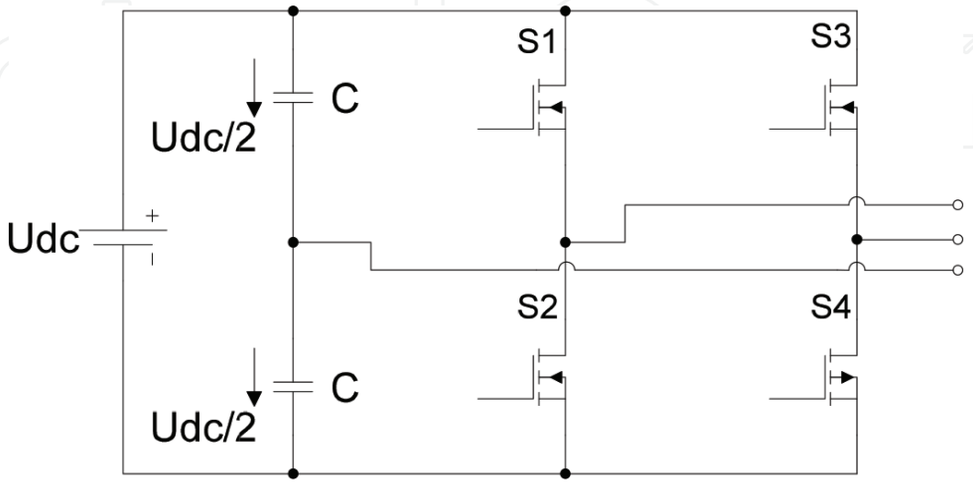

Figure 2. Voltage source inverter with two legs for supply of three-phase IM.

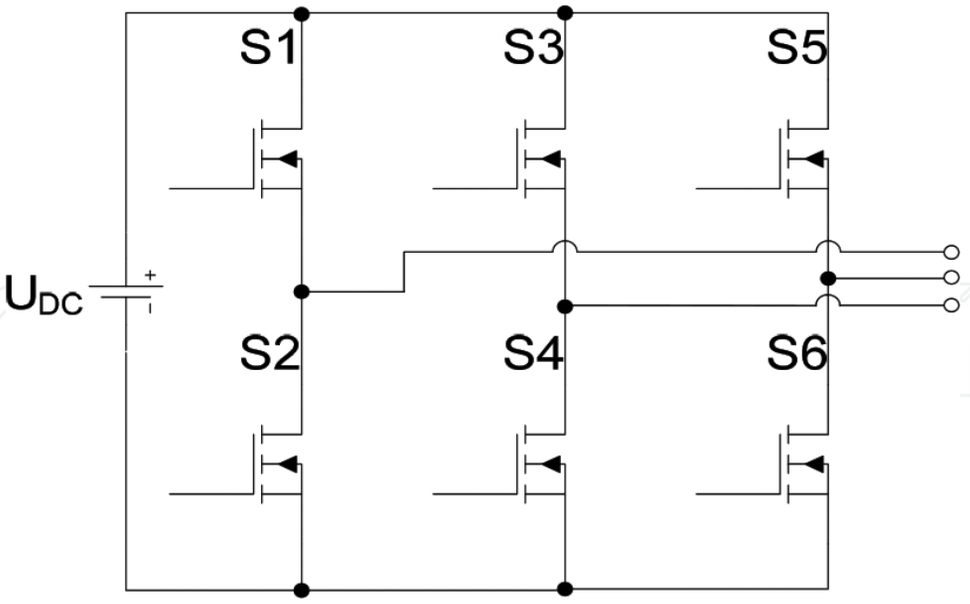

Figure 3. Voltage source inverter with three legs.

2.3. Two-phase voltage source inverter with four legs

Another possible topology that can be used to fed the two-phase induction motor (**Figure 4**) is created by eight switches. Each phase is fed by one full-bridge inverter.

The topology uses a larger amount of switches (eight ones), and therefore, the topology is able to use entire magnitude of DC interlink voltage [7, 21].

Model of two-phase IM motor is well known [7–9, 13, 14]. So, the electric machine being considered may be described by the following set of ordinary differential equations in the $\alpha\beta$-stator reference coordinate frame under the commonly used simplifying assumptions:

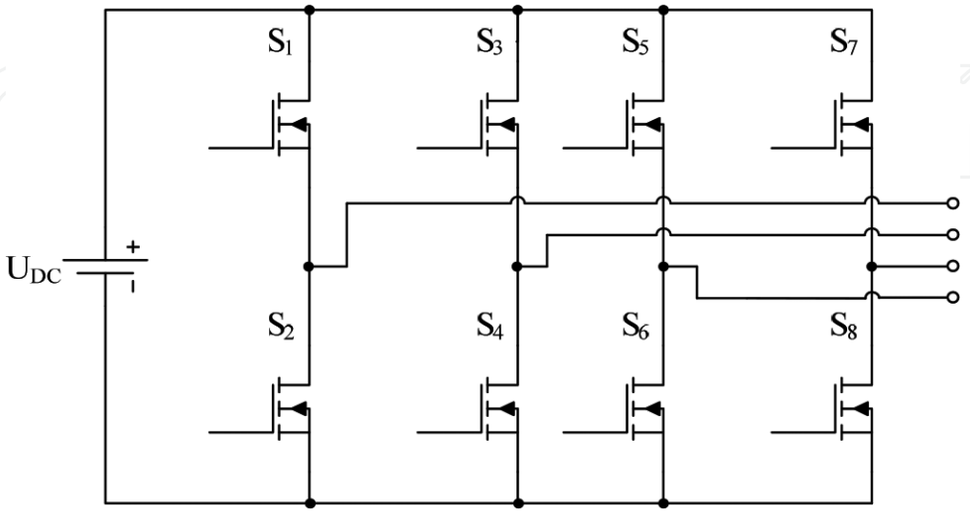

Figure 4. Voltage source inverter with four-leg and four-output terminals.

$$u_{s\alpha} = R_{s\alpha} i_{s\alpha} + L_{s\alpha} \frac{\mathrm{d}i_{s\alpha}}{\mathrm{d}t} + L_{M\alpha} \frac{\mathrm{d}i_{r\alpha}}{\mathrm{d}t}, \tag{1}$$

$$u_{s\beta} = R_{s\beta} i_{s\beta} + L_{s\beta} \frac{\mathrm{d}i_{s\beta}}{\mathrm{d}t} + L_{M\beta} \frac{\mathrm{d}i_{r\beta}}{\mathrm{d}t}, \tag{2}$$

$$0 = R_{r\alpha} i_{r\alpha} + L_{r\alpha} \frac{\mathrm{d}i_{r\alpha}}{\mathrm{d}t} + L_{M\alpha} \frac{\mathrm{d}i_{s\alpha}}{\mathrm{d}t} + + \frac{1}{N} \omega_m (L_{r\beta} i_{r\beta} + L_{M\beta} i_{s\beta}), \tag{3}$$

$$0 = R_{r\beta} i_{r\beta} + L_{r\beta} \frac{\mathrm{d}i_{r\beta}}{\mathrm{d}t} + L_{M\beta} \frac{\mathrm{d}i_{s\beta}}{\mathrm{d}t} + - N\omega_m (L_{r\alpha} i_{r\alpha} + L_{M\alpha} i_{s\alpha}), \tag{4}$$

$$T_e = pp \left[N(L_{r\alpha} i_{r\alpha} + L_{M\alpha} i_{s\alpha}) i_{r\beta} - \frac{1}{N} (L_{r\beta} i_{r\beta} + L_{M\beta} i_{s\beta}) i_{r\alpha} \right], \tag{5}$$

$$T_e = T_{\mathrm{load}} + J \frac{\mathrm{d}\omega_m}{\mathrm{d}t}. \tag{6}$$

where N is the ratio between the effective numbers of turns in the auxiliary and the main stator windings, ω_m is the mechanical angular speed, and pp is the number of pole pairs.

As control methods, it can be used modern control ones: field-oriented vector control as well as space vector pulse width modulation [6, 15]. Some results of operation of two-phase IM supply are shown in **Figure 5a**, start-up and steady state (b).

The topology VSI with two legs controlled by SVPWM is able to turn on a four active voltage vector but not able to turn on a zero voltage vector, which is its major disadvantage [21].

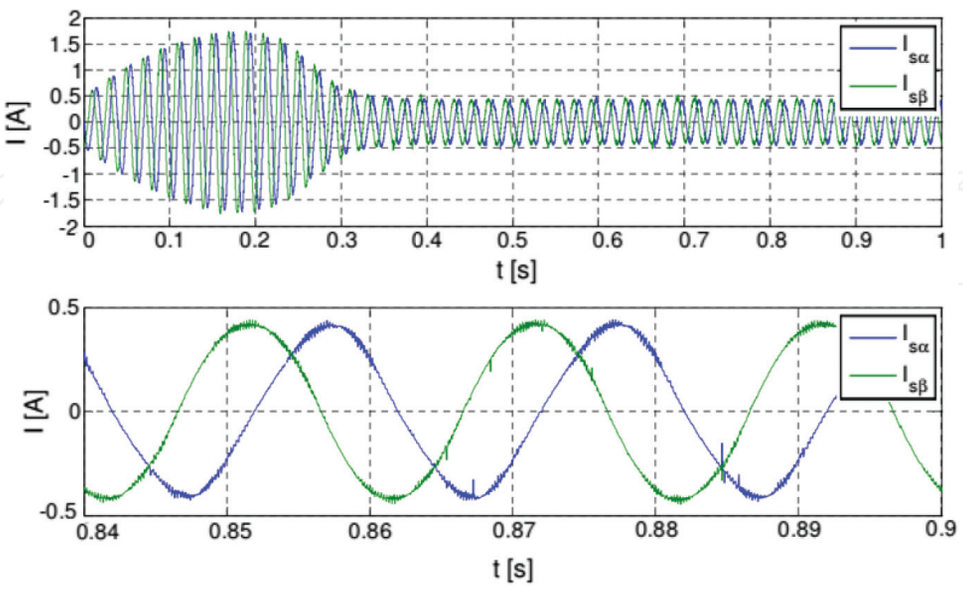

Figure 5. Behaviour of two-phase IM supplied by two-phase VSI inverter; (top) start-up and (bottom) steady-state operation [21].

Substituting VSI topology by matrix one will be able to turn on eight active voltage space vectors with turn-on times as shown in **Figure 6 (top)** but still no zero space vectors, **Figure 6 (bottom)**.

Instead of VSI inverters with two, three, and four legs, there can be used matrix converter [21], but the number of switching devices is rather higher, nearly two times.

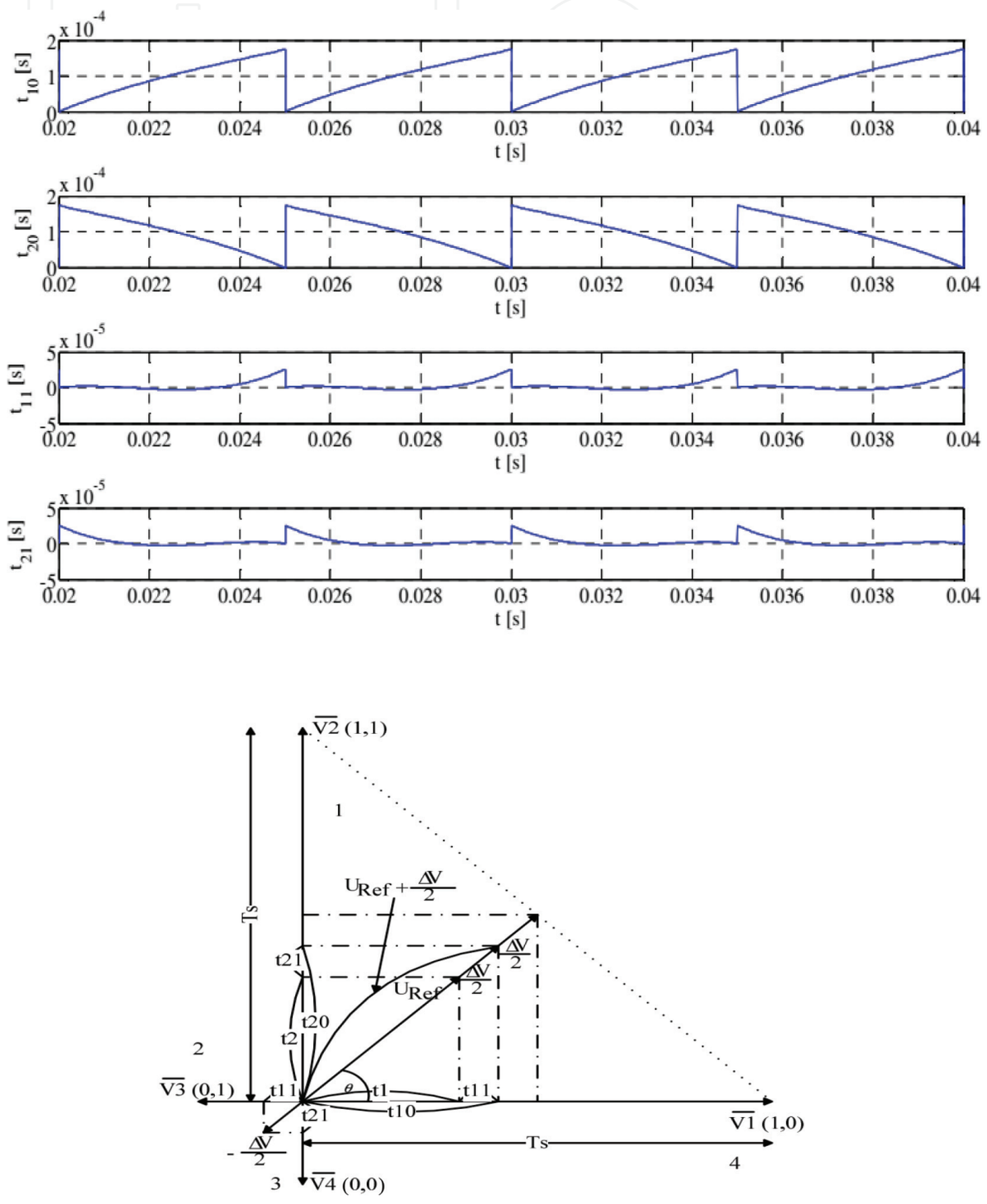

Figure 6. Two-leg VSI; (top) turn-on times of active voltage vectors and (bottom) creating SVPWM [21].

3. Two-phase inverters with minimum switching devices

3.1. Two-phase voltage source inverter with one leg

Minimum of switching devices: two switches for inverter, two diodes for rectifiers, are reached by the one-leg VSI inverter [8, 10], **Figure 7**.

Anyway, it also needs two antiparallel diodes and two bulky capacitors. Schematic of VSI in **Figure 7** is dedicated for ac motors. In full speed operation, the one leg of VSI with switches provides phase shift of 90°, since in reduced speed operation, the shift is created by a capacitor.

3.2. Two-phase voltage matrix converter with one and two legs

Instead of one-leg VSI inverters that can be used matrix converters is based on single-phase matrix converter. The matrix converter has some specific advantages over voltage source inverter in the size of the device, the lack of intermediate circuit, and also reduction in needed capacity [18]. The disadvantages are higher cost and also higher number of switching elements. Matrix converter that consists of just one single leg is described as original one, in Section 4.

3.3. Two-phase LCL2C2 inverter with two-leg matrix converter

One possibility for the first stage is to use a resonant converter, for instance an LCL2C2 resonant converter, **Figure 8a**. The second stage can be created as a two-leg two-phase matrix converter. This resonant converter consists of four bidirectional switches. For his control, an SVPWM modulation can be used, which is very like of SVPWM modulation for two-phase two-leg voltage VSI inverter.

The difference is the need to monitor the voltage polarity in an intermediate circuit and properly toggle the combination of active vectors. Unlike the two-phase two-leg voltage source

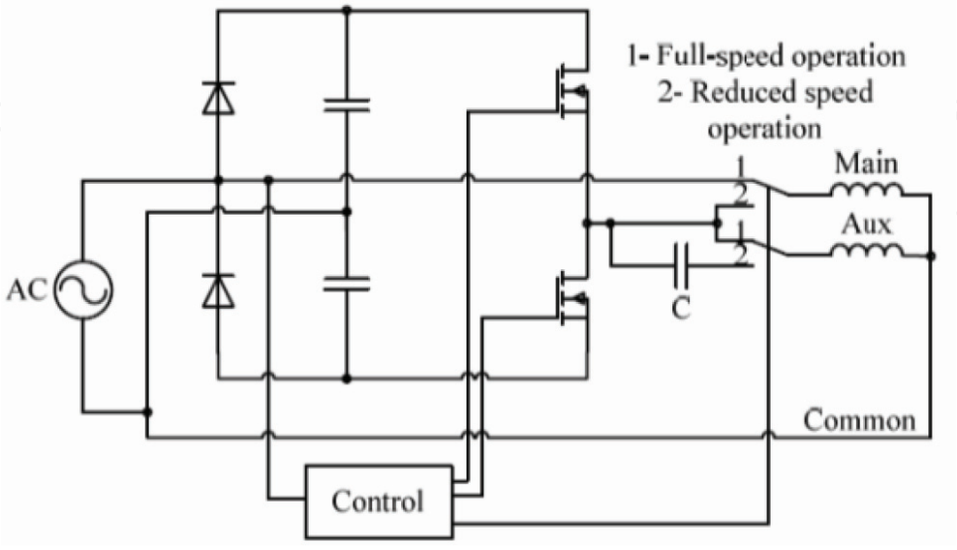

Figure 7. Schematic of one-leg VSI inverter [10].

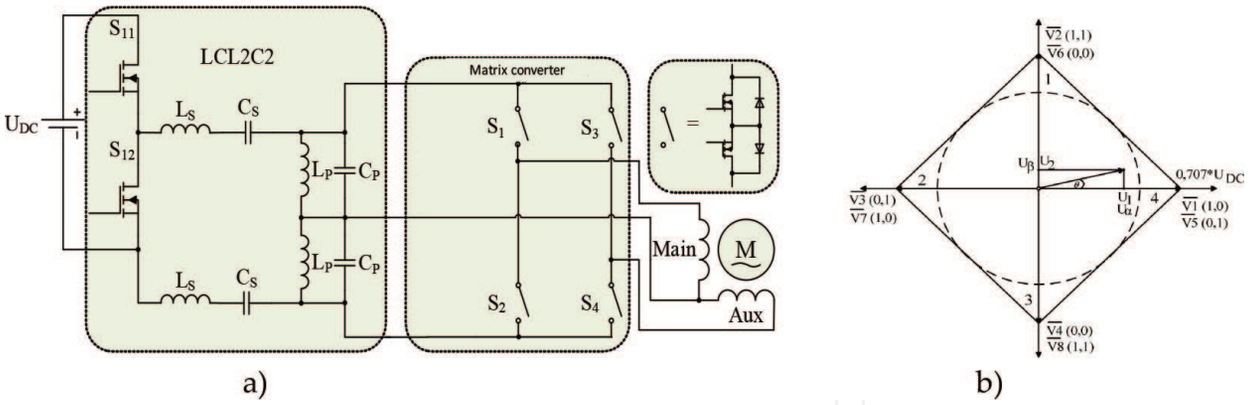

Figure 8. Two-stage MxC; (a) with resonant converter as a first stage and (b) its space vectors [21].

inverter, the two-phase two-leg matrix converter has double number of active vectors, **Figure 8b**. It is necessary to switch on the active vectors V1–V4 when the voltage in intermediate circuit is positive. If there is a negative voltage in the intermediate circuit, vectors V5–V8 are switched on. Reference voltage for the switches is shown in **Figure 9**.

The operation of matrix converter with motoric load in an open-loop operation and detail of stator currents and adequate stator voltages during two periods at steady state are shown in **Figure 10**.

Anyway, number of switching devices using two-phase LCL2C2 inverter with two-leg matrix converter is still high (2 + 4 that means six switches).

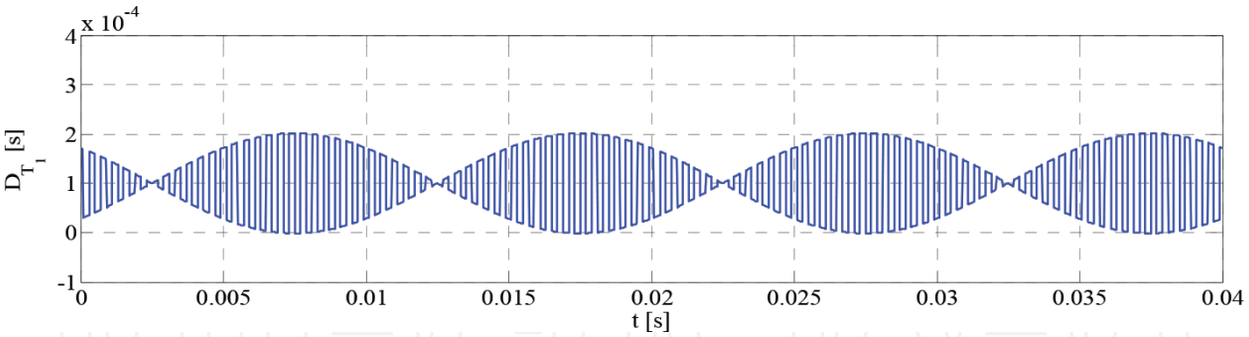

Figure 9. Waveforms of reference voltages for two-phase matrix converter [21].

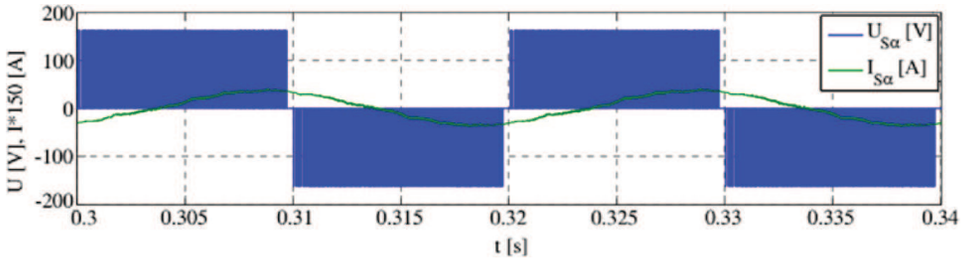

Figure 10. Stator voltages and stator currents of α-phase during two periods [21].

4. Single-leg topology using matrix converters for two-phase application

Another possibility how to reduce number of switching devices is presented by the special connection of one-leg matrix converter supplied direct from the network. As new type of two-phase converters using matrix converter for two-phase applications has been developed for single-leg matrix converter [17].

4.1. Basic topology of single-leg matrix converter

A novel supply system for two-phase induction motor by a single-leg matrix converter was introduced in work [17] using principle of *single-phase matrix converter where one phase is substituted by harmonic network voltage*, **Figure 11a** and **b**.

In the circuit operation of full speed regime, the voltage of auxiliary phase is possible to express as

$$u_{\text{aux}}(t) = U_M \text{sign}[\sin(\omega t)]\text{abs}[\cos(\omega t)]. \tag{7}$$

For reduced speed, the voltage of both main and auxiliary phases is expressed as

$$u_{\text{mxc}}(t) = U_M \text{sign}[N \sin(\omega t)]\text{abs}[\sin(\omega t)], \tag{8}$$

$$N = \frac{f_{mxc}}{f_{ac}} = \frac{T_{ac}}{T_{mxc}}. \tag{9}$$

The input and output waveforms of MxC in full speed mode and reduced speed mode are shown in **Figures 12** and **13**. The switching logic of the control system that creates the desired output voltage from input voltage is shown in **Figure 14**.

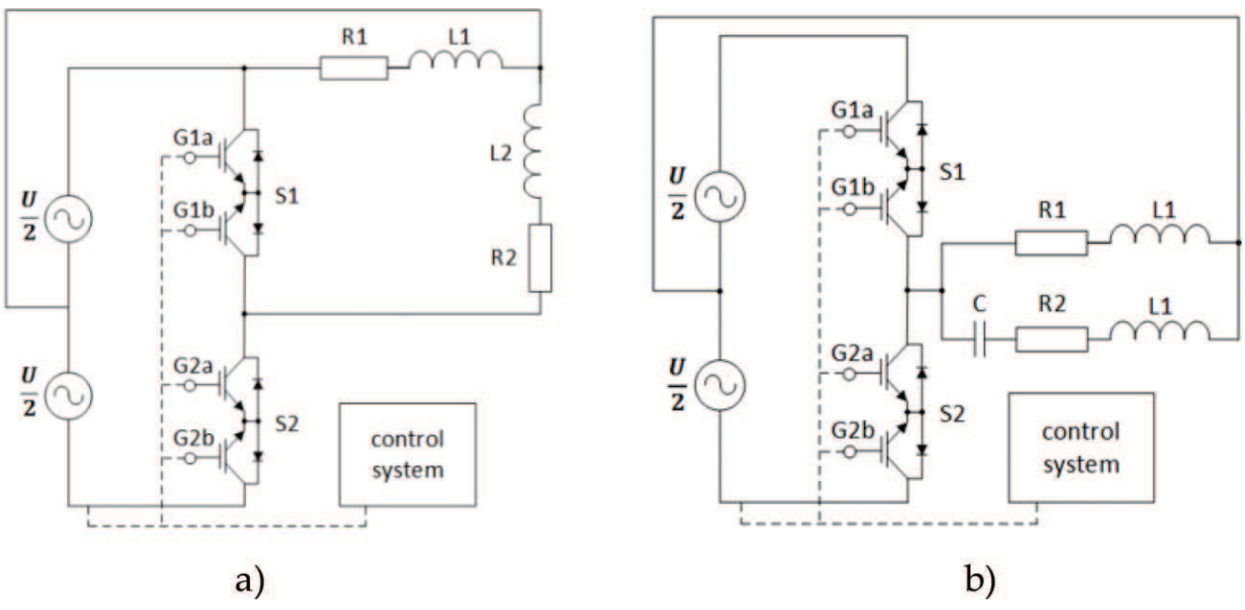

Figure 11. One-Leg MxC; (a) schematics for full speed at 50 Hz and (b) for reduce speed (<50 Hz) [17].

Among various questions, the first question is how value of the fundamental harmonic of auxiliary phase will reached. Using Fourier analysis of the one fourth of the waveform, **Figure 15**, one can write equations:

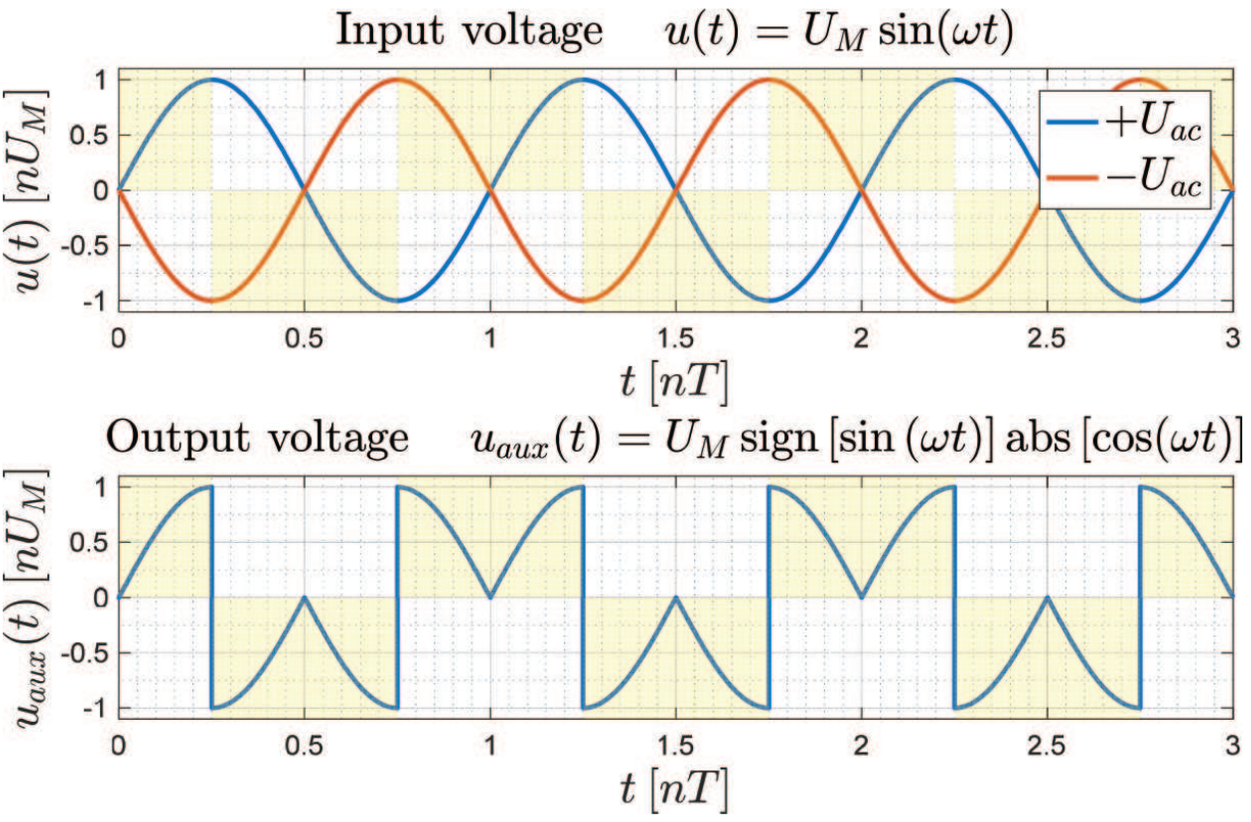

Figure 12. Voltages of SLMxC in full speed mode 50 Hz; (top) input network voltage and (bottom) SLMxC output voltage.

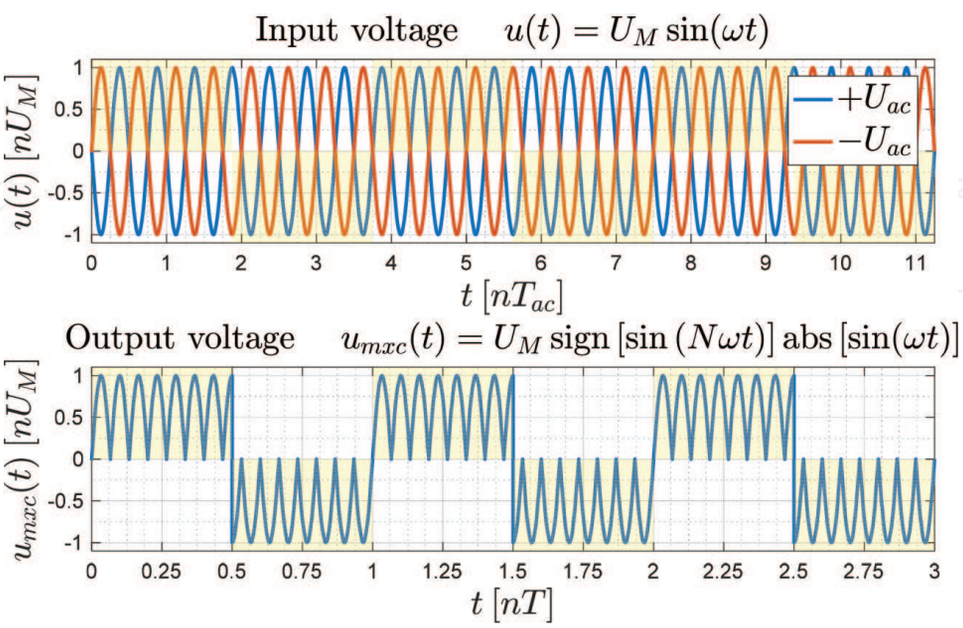

Figure 13. Voltages of SLMxC in reduced speed mode 6.66 Hz; (top) input and (bottom) output voltages.

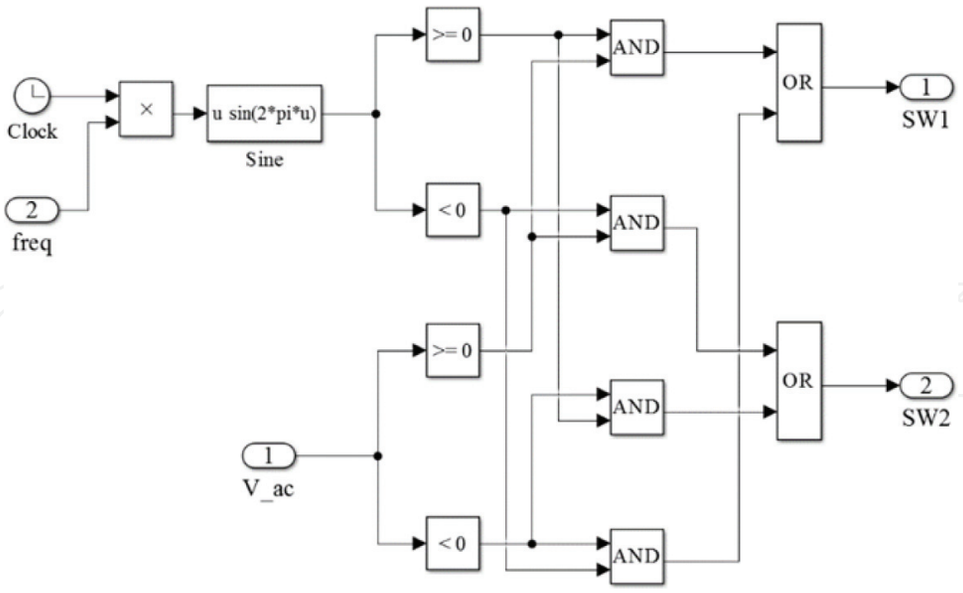

Figure 14. The switching logic for main and auxiliary phases.

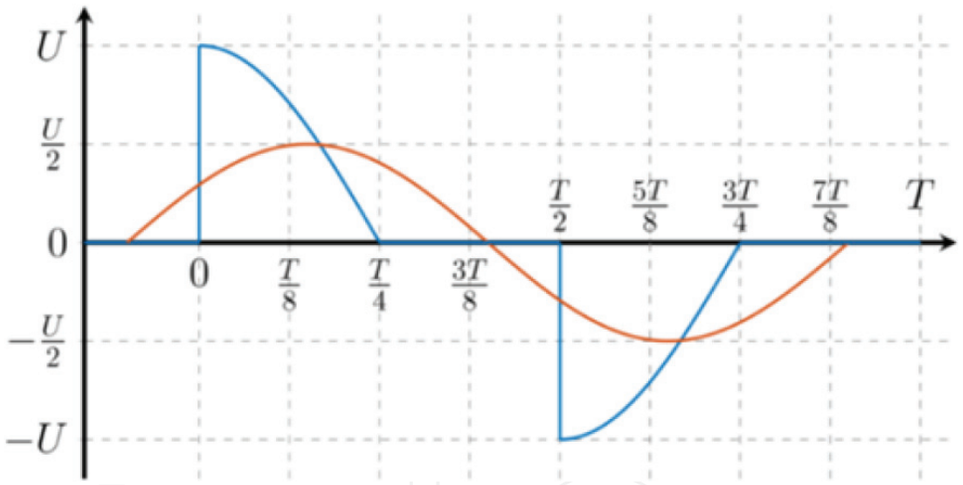

Figure 15. To harmonic analysis for the first part of the waveform.

Definite relations

$$f_1(t) = a_1 \cos(\omega_1 t) + b_1 \sin(\omega_1 t) = A_1 \sin(\omega_1 t + \varphi_1), \tag{10}$$

$$A_1 = \sqrt[2]{{a_1}^2 + {b_1}^2};\ \varphi_1 = \operatorname{arctag} \frac{b_1}{a_1}, \tag{11}$$

$$a_1 = \frac{2}{T}\int_0^T f(t)\cos(\omega_1 t)\mathrm{d}t;\ b_1 = \frac{2}{T}\int_0^T f(t)\sin(\omega_1 t)\mathrm{d}t. \tag{12}$$

Then

$$a_1 = \frac{2}{T}\int_0^{\frac{T}{4}} \cos^2(\omega_1 t)\mathrm{d}t = \frac{2}{T}\int_0^{\frac{T}{4}} \frac{1}{2}[1 + \cos(2\omega_1 t)]\mathrm{d}t$$
$$= \frac{1}{T}\int_0^{\frac{T}{4}} [1 + \cos(2\omega_1 t)]\mathrm{d}t = \frac{1}{T}[t]_0^{T/4} + \frac{1}{T}\frac{1}{2\omega_1}[\sin(2\omega_1 t)]_0^{T/4} = \frac{1}{4}, \tag{13}$$

$$b_1 = \frac{4}{T}\int_0^{T/2} f(t)\sin(\omega_1 t) = \frac{2}{T}\int_0^{\frac{T}{4}} \cos(\omega_1 t)\sin(\omega_1 t)\mathrm{d}t$$
$$= \frac{2}{T}\int_0^{\frac{T}{4}} \frac{1}{2}[\sin(2\omega_1 t)]\mathrm{d}t = \frac{1}{T}\frac{1}{2\omega_1}[-\cos(2\omega_1 t)]_0^{T/4} = \frac{1}{4\pi}[\cos(2\omega_1 t)]_{T/4}^0 = \frac{1}{2\pi}. \tag{14}$$

Fundamental harmonic waveform

$$u_1(t) = \frac{1}{4}\cos(\omega_1 t) + \frac{1}{2\pi}\sin(\omega_1 t) = \sqrt[2]{\left(\frac{1}{4}\right)^2 + \left(\frac{1}{2\pi}\right)^2}\sin\left(\omega_1 t + \operatorname{arctag}\frac{1/2\pi}{1/4}\right). \tag{15}$$

After calculation

$$u_1(t) = 0.296\sin(\omega_1 t + 32.48^\circ). \tag{16}$$

The value if fundamental harmonic at the middle of half-period

$$A_1|_{\frac{\pi}{2}} = 0.296\cos(32.48^\circ) = 0.249. \tag{17}$$

The contribution from the second part of auxiliary-phase waveform will be the same, **Figure 16**. So, this means that maximal magnitude of auxiliary-phase fundamental harmonic is

$$2A_1|_{\frac{\pi}{2}} = 2 \times 0.249 = 0.498 \approx 0.5. \tag{18}$$

Thus, the RMS value of the output voltage of the one-leg converter should be two times greater than requested voltage of the main phase of the system.

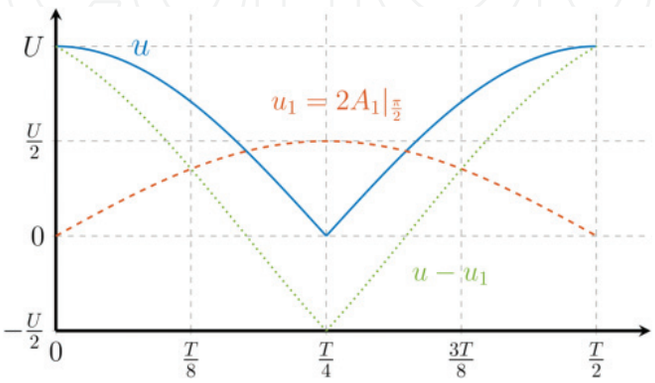

Figure 16. Auxiliary-phase waveforms; (solid) total wave, (dashed) fundamental harmonic and (dotted) sum of higher harmonics.

Basic scheme of MxC converter for reduced speed is different from full speed and given in **Figure 11b**. The phase shift of auxiliary phase is provided by the capacitor C_{aux}. Vector diagram for auxiliary-phase impedances is given in **Figure 17**.

By calculating C_{aux} for 'quadratic mean' frequency band 33.33 Hz from vector diagram, the capacitor value for auxiliary phase can be determined

$$|Z_{aux}| = |Z_{main}|,\ f_{qm} = \sqrt{\frac{f_{lo}^2 + f_{hi}^2}{2}}, \tag{19}$$

$$\left|\frac{1}{\omega C_{aux}}\right| = |Z_{aux}|\cos\varphi + |\omega L_2|, \tag{20}$$

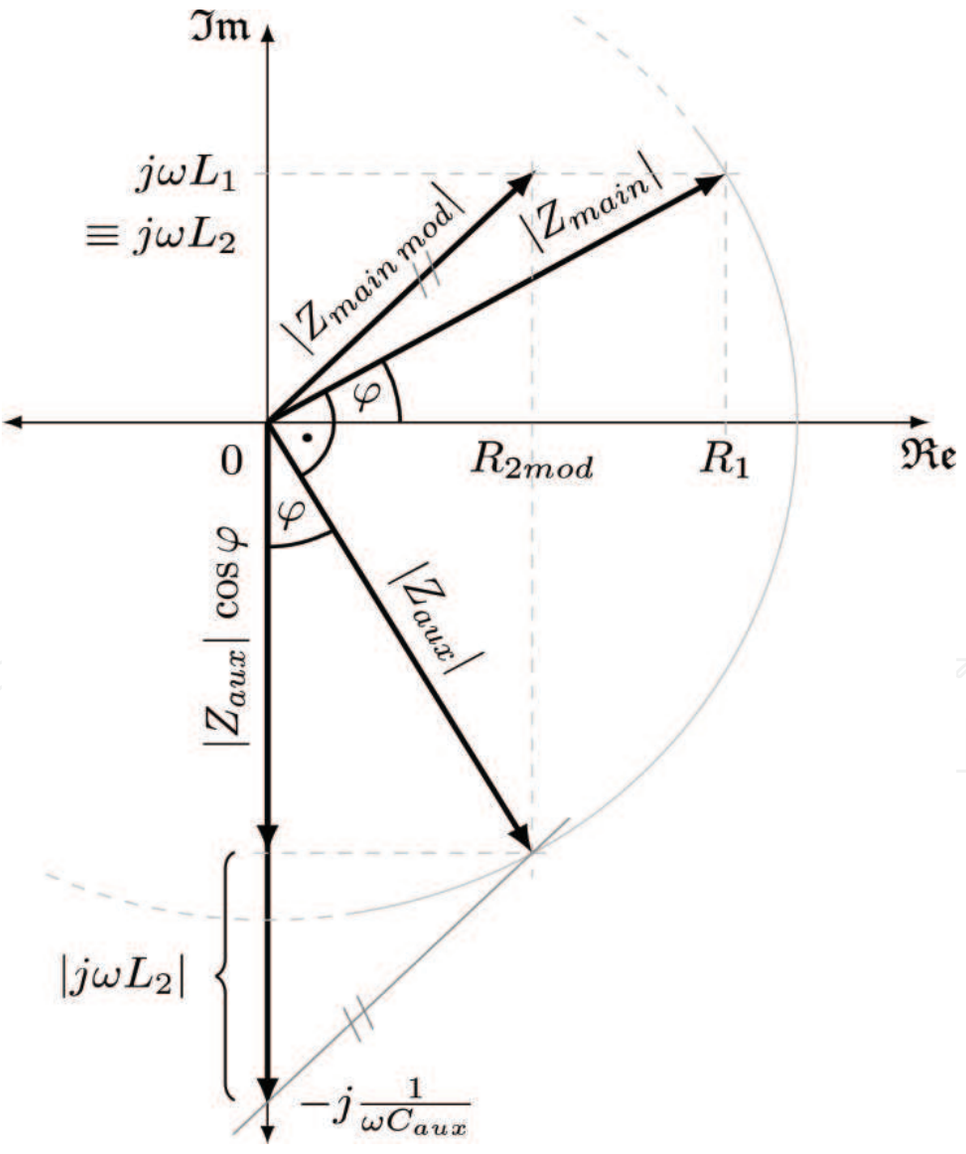

Figure 17. Vector diagram for reduce speed of auxiliary-phase impedances.

$$C_{\text{aux}} = \frac{1}{\omega} \frac{1}{|Z_{\text{aux}}| \cos\varphi + |\omega L_2|}. \tag{21}$$

There is equality of $|\omega L_2| = |\omega L_1|$ to be the same magnetic flux in both main and auxiliary phases.

Analytical differential equations for main- and auxiliary-phase state-space variables (**Figure 11b**) are:

$$\frac{\mathrm{d}i_{\text{main}}}{\mathrm{d}t} = -\frac{1}{\tau} i_{\text{main}} + \frac{1}{\tau} \frac{U_m}{R_1} \sin(\omega t), \tag{22}$$

$$\frac{\mathrm{d}i_{\text{aux}}}{\mathrm{d}t} = -\frac{1}{\tau} i_{\text{aux}} + \frac{1}{L_1} u_C + \frac{1}{\tau} \frac{U_m}{R_2} \sin(\omega t), \tag{23}$$

$$\frac{\mathrm{d}u_C}{\mathrm{d}t} = \frac{1}{C} i_{\text{aux}}, \tag{24}$$

where τ is time constant accordingly R_1 and R_2 resistances.

After time discretization (e.g. using Euler's method), we obtain discrete dynamic model suitable for simulation in Matlab/Simulink.

Similar to one-leg VSI inverter [8, 12], the number of switches of single-leg MxC is minimized but total harmonic distortion auxiliary-phase voltage is very high (86% at 50Hz, 69% at 33.33 Hz) and consequently current distortions too (68% and 43%, respectively), see **Figure 18** in Section 6 for simulation results where **Figure 18a** is for 50 Hz and **Figure 18b** is for 33.33 Hz.

4.2. Single-leg matrix converter supplying IM without LC filter and PWM

Due to very high THD of the main and auxiliary voltages and current, there is a problem regarding to electromagnetic torque generated by two-phase IM motor. Therefore, neither the operation at 50 Hz nor at reduced frequency (33.33 or 25 Hz), under nominal torque and during start-up, could be provided successfully.

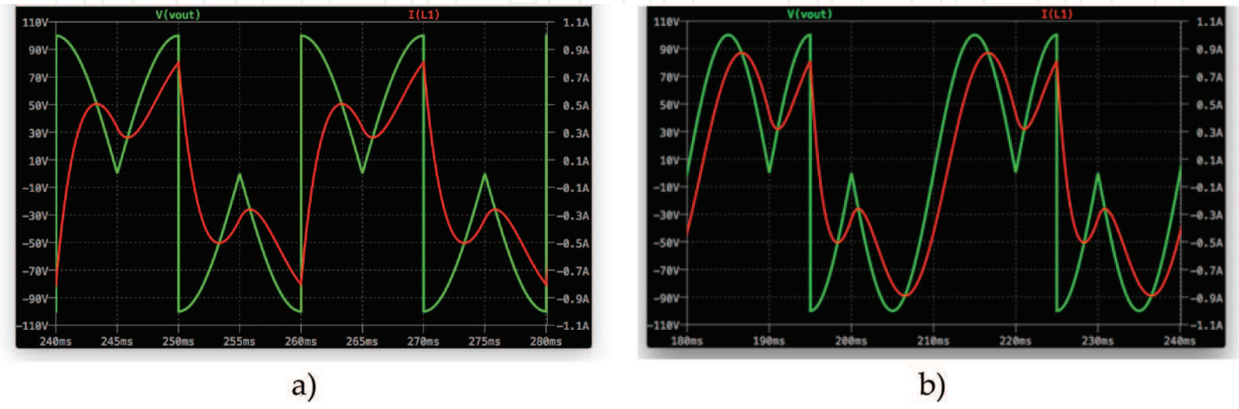

a) b)

Figure 18. One-Leg MxC; (a) voltage and current of auxiliary-phase at 50 Hz and (b) at 33.33 Hz.

Thus, we have to accept some measures for successfully operating PWM control, adding LC resonant filter, and/or using switched capacitor.

Parameters of the two-phase IM used for simulation are therefore given in Section 5 with PWM controlled motor.

4.3. Improving single-leg matrix converter using LC filter

Thus, it is necessary to improve current waveforms. Current-controlled PWM modulation (CC-PWM) for full-speed operation is not possible to use because of decreasing of auxiliary-phase voltage. Other possibility that has been used is using of LC resonant circuit that can be used both in auxiliary and main-phase circuits, **Figure 19a** and **b**.

Analytical differential equations for main- and auxiliary-phase state-space variables (**Figure 19b**)

$$\frac{\mathrm{d}i_{\mathrm{main}}}{\mathrm{d}t} = -\frac{1}{\tau} i_{\mathrm{main}} + \frac{1}{L_1} u_{\mathrm{Cres}} + \frac{1}{\tau} \frac{U_m}{R_1} \sin(\omega t), \tag{25}$$

$$\frac{\mathrm{d}i_{\mathrm{aux}}}{\mathrm{d}t} = -\frac{1}{\tau} i_{\mathrm{aux}} + \frac{1}{L_{2\mathrm{mod}}} u_C + \frac{1}{\tau} \frac{U_m}{R_{2\mathrm{mod}}} \sin(\omega t), \tag{26}$$

$$\frac{\mathrm{d}u_{\mathrm{Cres}}}{\mathrm{d}t} = \frac{1}{C_{\mathrm{res}}} \, i_{\mathrm{main}}, \tag{27}$$

$$\frac{\mathrm{d}u_C}{\mathrm{d}t} = \frac{1}{C_{\mathrm{aux}}} \, i_{\mathrm{aux}}, \tag{28}$$

where τ is time constant accordingly to R_1 and R_2 resistances, and C_{aux} is series connected C and C_{res} capacitors.

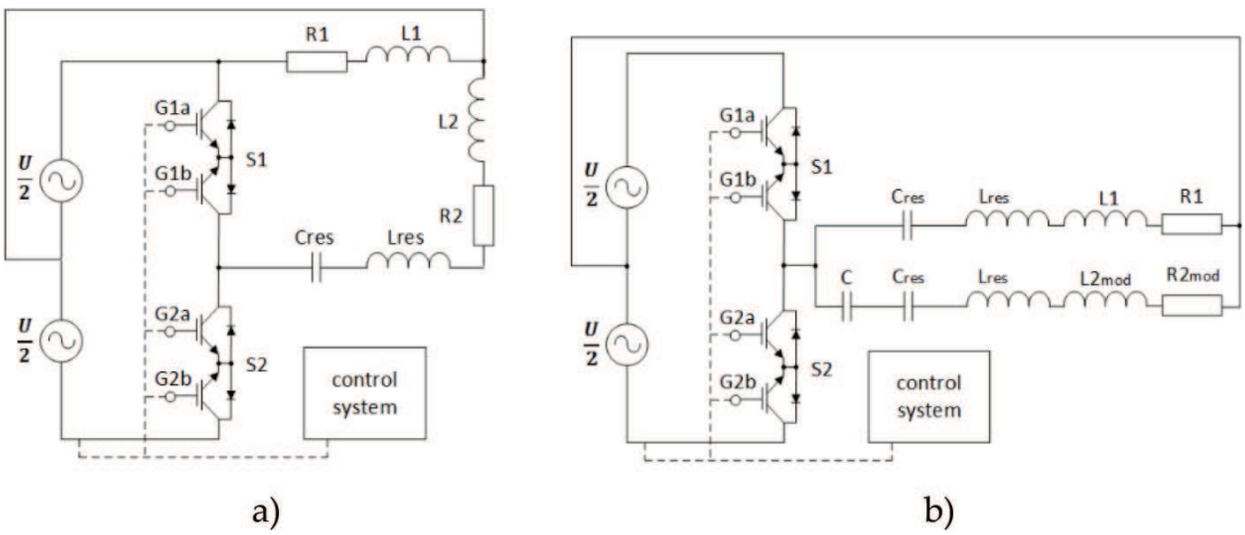

Figure 19. Schematics of SLMxC; (a) for full speed at 50 Hz and (b) for reduce speed (<50 Hz) with LC circuits.

After time discretization (e.g. using Euler's method), we obtain discrete dynamic model suitable for simulation in Matlab/Simulink.

After realization of above measures, the total harmonic distortion of main and auxiliary-phase currents will be much better such as 12.47% at 50 Hz and 8.47% at 33.33 Hz with LC circuits, see **Figure 20a** for 50 Hz and **Figure 20b** for 33.33 Hz in Section 6. By suitable design of LC elements [20], it is possible to reach the best value of main-and auxiliary-phase current THDs (<5%) but the size of the LC elements will be rather high.

Resonant LC filter can be tuned either for given frequency 50 Hz, schematic in **Figure 19a**, or for 'quadratic mean' frequency band 33.33 Hz, schematic in **Figure 19b**. Design of LC filter has been done using design procedure by Dobrucký et al. [20].

4.4. Improving single-leg matrix converter by combining switched capacitors and LC filter

Auxiliary-phase advancing using switched C or L elements can be provided by different ways [13, 14]

- switched capacitor with four switches networks, **Figure 21a**

- switched capacitors with two switches and two capacitors, **Figure 21b**

- switched RLC (inductor and capacitor) circuit with two switches connected as series network, **Figure 21c**

- switched inductor with two switches connected as parallel network, **Figure 21d**

Since first two possibility items operate with full controlled bidirectional switches the later two can be operated by ordinary thyristors with uncontrolled switching-off of the circuit current.

A periodically reversed switched capacitor is connected in series with an RL load supplied from a sinusoidal voltage source. To control the phase of the fundamental component of load current, a suitable algorithm for the switching of the capacitor is derived and tested. The operation of the switch pairs is complementary and supports a pulse width modulated regime where the duty factor of the dominant pair, e.g. S1, is restricted to vary between 0.5 and unity.

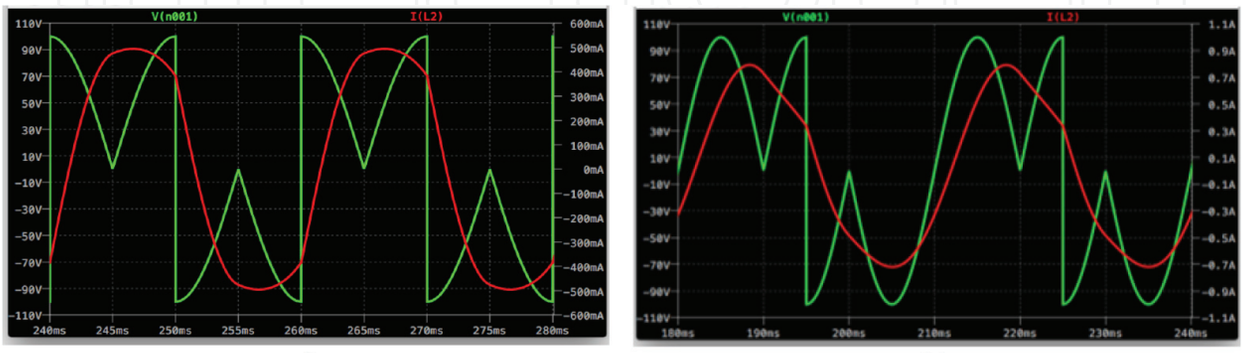

Figure 20. Voltage and current of auxiliary-phase at 50 Hz (a) and at 33.33 Hz (b) with additional LC circuit.

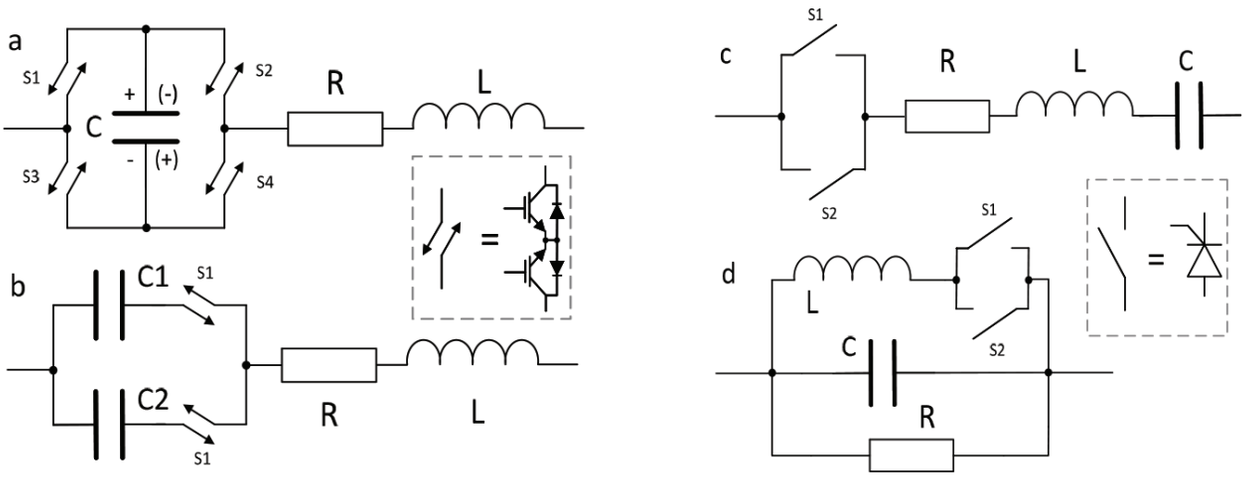

Figure 21. Possibilities of switched capacitor networks for phase shift control.

We have chosen a variant shown in **Figure 21b** because of variant **Figure 19a** that needs high number of switches and variants **Figure 19c** and **d** operate with uncontrolled switching-off of the circuit current only, with an auxiliary winding through the bidirectional choppers S1 and S2 controlled by PWM with a frequency of about 1 kHz. The capacitance is changed by variation of the duty cycle

$$D_{\mathrm{tc}} = \frac{t_{\mathrm{on}}}{t_{\mathrm{on}} + t_{\mathrm{off}}}, \tag{29}$$

from 0 to 1.

The switches S1, S2 are linked with each other by an inverted logic. One capacitor has high capacitance and the other has low capacitance. The desired capacitance is set as a function of duty cycle for the switching between these two capacitors.

The equation for the controlled switched capacitance C can be derived from the energy stored in the capacitors [8]

$$E = \frac{1}{2} C U^2. \tag{30}$$

From Fourier analysis, the dc component of periodic waveform is equal to its average value

$$U_{\mathrm{s}} = \frac{1}{\mathrm{T}} \int_0^T \mathrm{u(t)d}t = D_{\mathrm{tc}}\, U, \tag{31}$$

where D_{tc} is the duty cycle and T is the switching period. Therefore, the average voltages on the capacitors are

$$U_1 = D_{\mathrm{tc}}\, U,\ U_2 = (1 - D_{\mathrm{tc}})\, U. \tag{32}$$

Then, the total energy stored in the two capacitors is

$$\frac{1}{2}CU^2 = \frac{1}{2}C_1U_1^2 + \frac{1}{2}C_2U_2^2. \tag{33}$$

Thus,

$$CU^2 = C_1(D_{tc}U)^2 + C_2[(1 - D_{tc})U]^2. \tag{34}$$

After further simplification, we get the final equation for the switched capacitance as the function of duty cycle

$$C = C_1{D_{tc}}^2 + C_2(1 - D_{tc})^2. \tag{35}$$

The absolute value of the auxiliary impedance $|Z_{aux}|$ and the phase angle φ used in the function calculations are given as

$$|Z_{aux}| = \sqrt{R_{2mod}^2 + (\omega L_2)^2}, \tag{36}$$

$$\varphi = \tan^{-1}\frac{\omega L_2}{R_2}. \tag{37}$$

Combining Eq. (21) for the auxiliary-phase capacitance C_{aux} with Eq. (35) for switched capacitance $C_{aux} = C$ yields

$$0 = (C_1 + C_2){D_{tc}}^2 - 2C_2D_{tc} + C_2 - C_{aux}(\omega), \tag{38}$$

and

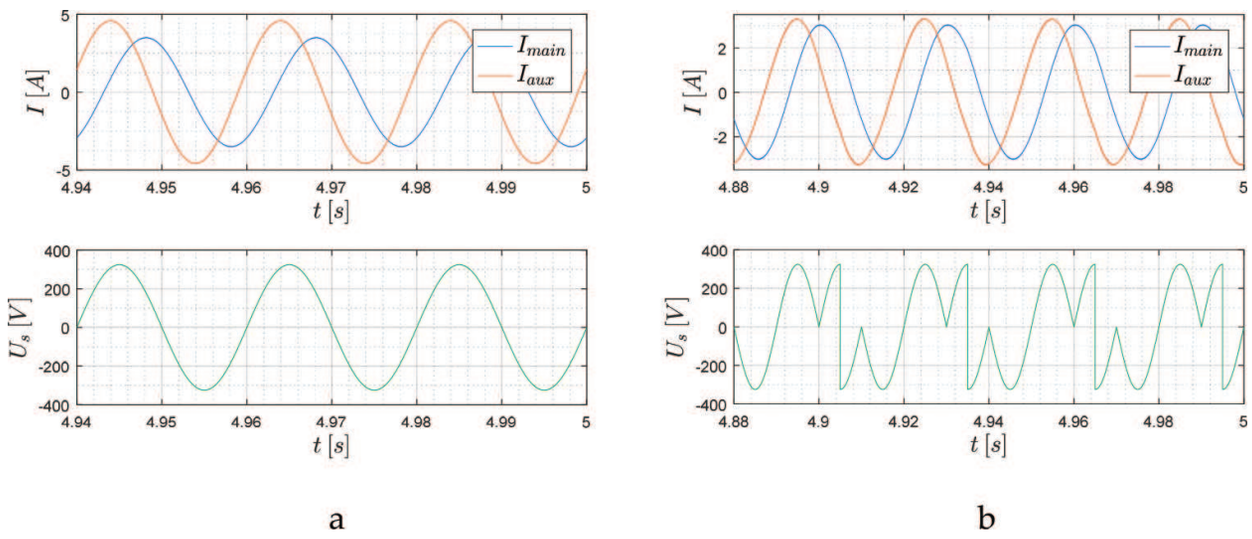

Figure 22. Main- and auxiliary-phase steady-state current (top) and SLLC MxC output voltage (bottom); (a) at 50 Hz and (b) at 33.33 Hz.

$$0 = (C_1 + C_2){D_{\text{tc}}}^2 - 2C_2D_{\text{tc}} + C_2 - \frac{1}{\omega}\frac{1}{|Z_{\text{aux}}|\cos\varphi + |\omega L_2|}. \tag{39}$$

Finding the roots of the quadratic equation we get the duty cycle D_{tc} as a function of the angular frequency ω that we can use for controlling the phase shift of the auxiliary phase

$$D_{\text{tc}}(\omega) = \frac{C_2 - \sqrt{C_{\text{aux}}(\omega)\ (C_1 + C_2) - C_1\,C_2}}{C_1 + C_2}. \tag{40}$$

In a similar way, we can derive a switching capacitor for the resonant filters, L_{res} and C_{res}. From the resonant frequency equation, we can calculate the value of resonant capacitance

$$C_{\text{res}} = \frac{1}{L\ \omega_{\text{res}}^2}. \tag{41}$$

Again, combining Eq. (41) for resonant capacitance with Eq. (35) for the switching capacitance $C_{\text{res}} = C$ yields

$$0 = (C_1 + C_2){D_{\text{tc}}}^2 - 2C_2D_{\text{tc}} + C_2 - C_{\text{res}}(\omega), \tag{42}$$

and

$$0 = (C_1 + C_2){D_{\text{tc}}}^2 - 2C_2D_{\text{tc}} + C_2 - \frac{1}{L_{\text{res}}\ \omega_{\text{res}}^2}. \tag{43}$$

On solving the equation, we get similar equation for control of resonant frequency

$$D_{\text{tc}}(\omega) = \frac{C_2 - \sqrt{C_{\text{res}}(\omega)\ (C_1 + C_2) - C_1\,C_2}}{C_1 + C_2}. \tag{44}$$

Switched capacitor will provide a requested phase shift of 90°. Requested waveforms shape should be provided by an additional LC resonant filter [19].

4.5. Single-leg matrix converter combining switched capacitors and LC filter supplying IM

Accepting of measures mentioned in Sections 4.3 and 4.4, it is possible essentially to improve quality of SLMxC. Combining switched capacitor in auxiliary phase and using LC resonant filter between the center tape of SLMxC and neutral point, it will be possible to obtain demanded current waveforms with lower value of total harmonic distortion of both main and auxiliary phases.

Worked-out simulation results are given in Section 6. At first, the simulation results of SLMxC with switched capacitors and LC filter under RL load are given in **Figure 22a** for 50 Hz, **Figure 22b** for 33.33 Hz, **Figure 23a** for 25 Hz and **Figure 23b** for 10 Hz.

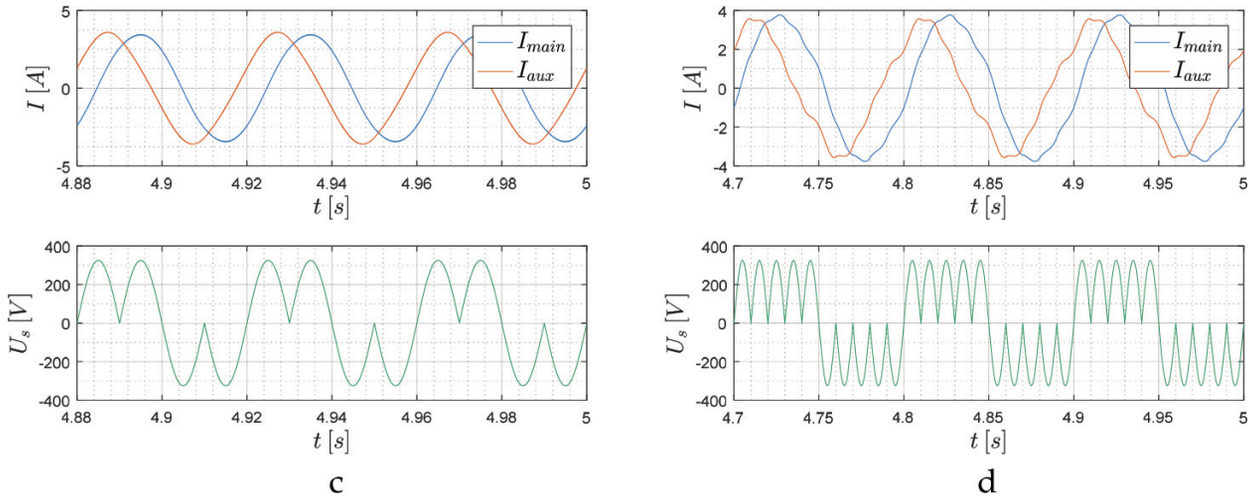

Figure 23. Main- and auxiliary-phase steady-state current (top) and SLLC MxC output voltage (bottom) at 25 Hz (c), and 10 Hz (d).

Simulation results of SLMxC with switched capacitors and LC filter under motoric IM load are shown in **Figures 24–26** in Section 6. There are shown steady-state currents and voltages of main and auxiliary phases in **Figure 24** at 50 Hz, in **Figure 25** at 33.33 Hz with PWM control, and also start-up operation in **Figure 26**.

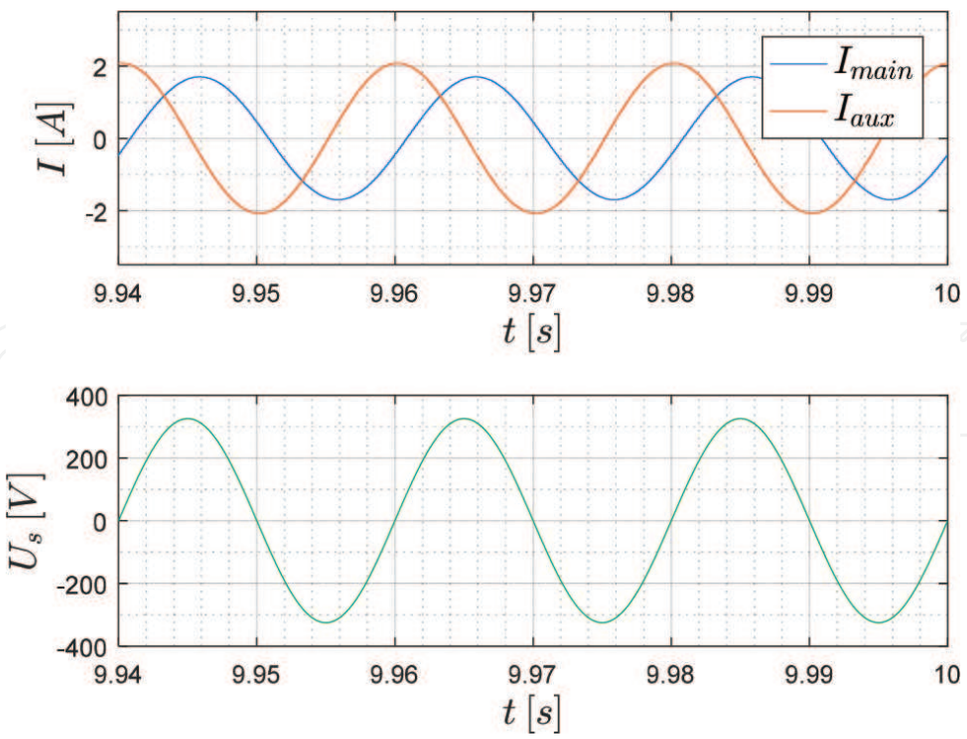

Figure 24. Main- and auxiliary-phase steady-state current of two-phase IM (top) and SLLC MxC output voltage (bottom) at 50 Hz without PWM.

http://dx.doi.org/10.5772/67743

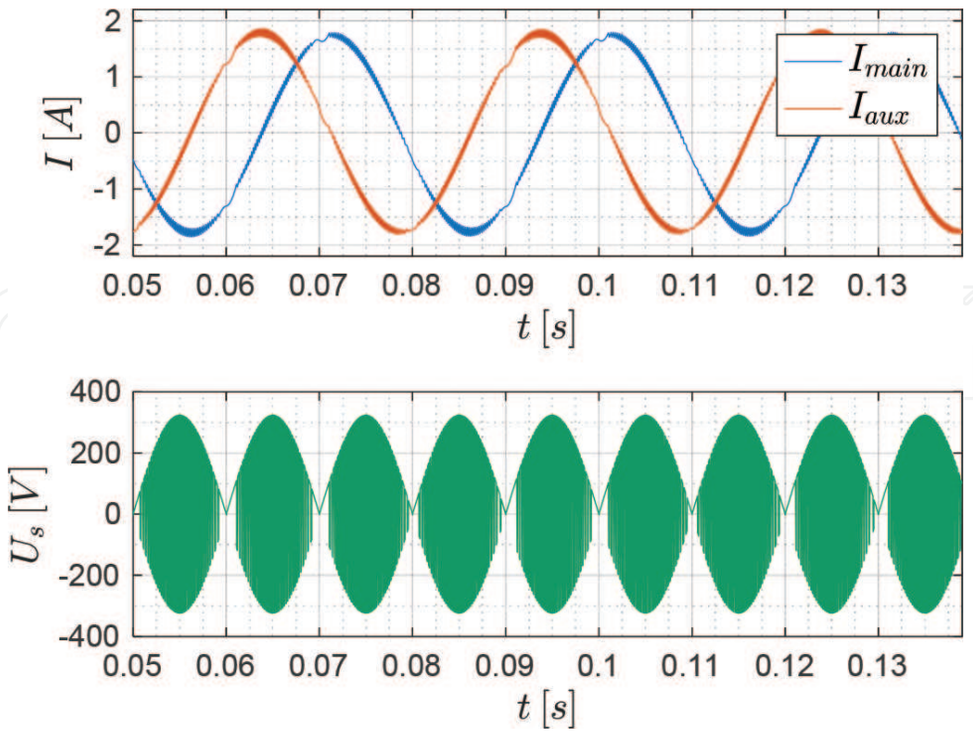

Figure 25. Main- and auxiliary-phase steady-state current of two-phase IM (top) and SLLC MxC output voltage (bottom) at 33.33 Hz with PWM.

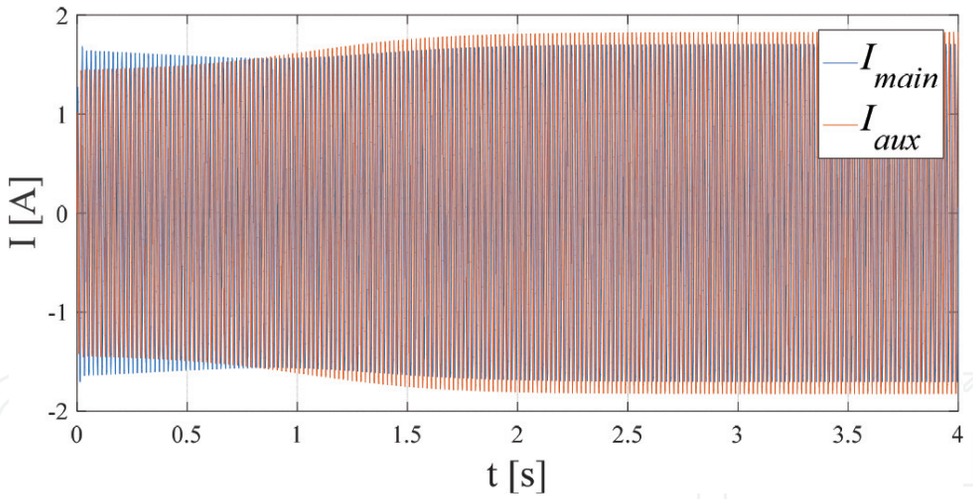

Figure 26. Main- and auxiliary-phase current of two-phase IM supplied by SLLC MxC during start-up.

5. Current controlled PWM for single-leg topologies

5.1. Current control of single-phase induction motor fed by single-leg VSI voltage source inverter

Simulation results, **Figure 27**, were worked-out without LC filter and switched capacitor [15].

Parameters used for the simulation with an induction machine:

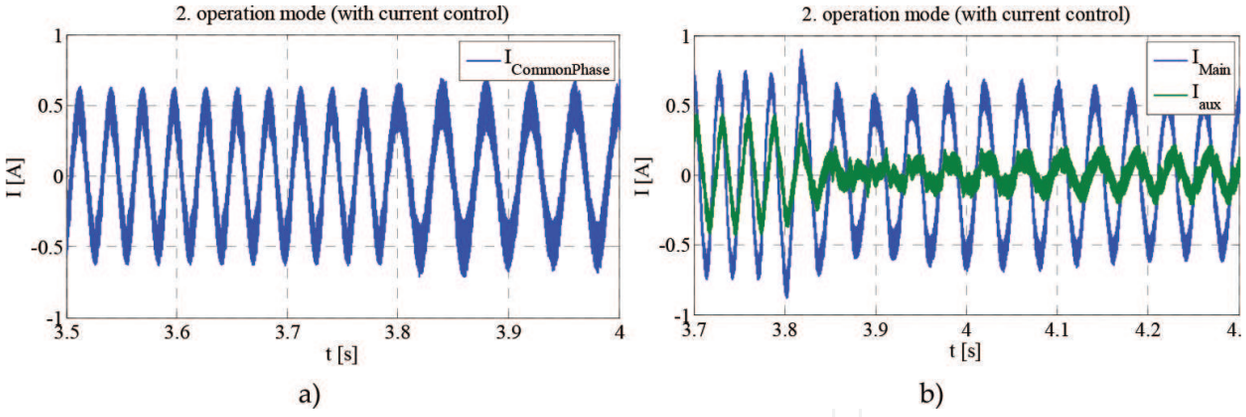

Figure 27. Currents controlled by hysteresis control; (a) in common phase and (b) in auxiliary phase [15].

$f = 50$ Hz; $U_{\text{rms}} = 230$ V; $P_{\text{av}} = 150$ W; $R_{\text{main}} = 58,85$ Ω; $R_{\text{aux}} = 66,1$ Ω; $L_{\text{main}} = 95$ mH; $L_{\text{aux}} = 120$ mH; M= 250 mH; and $C_{\text{aux}} = 20$ μF.

It can be seen that the waveforms of currents of main and auxiliary phases are not shaped sufficiently. Further improving would be possible using mentioned measures, i.e. LC filter and switched capacitor.

5.2. Current control of single-phase induction motor fed by basic single-leg MxC

Basic single-leg MxC schematic is given in **Figure 11a** and **b**. As mentioned in Section 4.2, there is a problem regarding to an electromagnetic torque generated by two-phase IM motor due to very high THD of the main and auxiliary voltages and current. Therefore, neither the operation at 50 Hz nor at reduced frequency (33.33 or 25 Hz), under nominal torque and during start-up, could be provided successfully.

Parameters used for the simulation with the induction machine (the same as above):

$f = 50$ Hz; $U_{\text{rms}} = 230$ V; $P_{\text{av}} = 150$ W; $R_{\text{main}} = 58,85$ Ω; $R_{\text{aux}} = 66,1$ Ω; $L_{\text{main}} = 95$ mH; $L_{\text{aux}} = 120$ mH; M= 250 mH; and $C_{\text{aux}} = 20$ μF.

Simulation results without LC filter and switched capacitor are given in **Figure 28**.

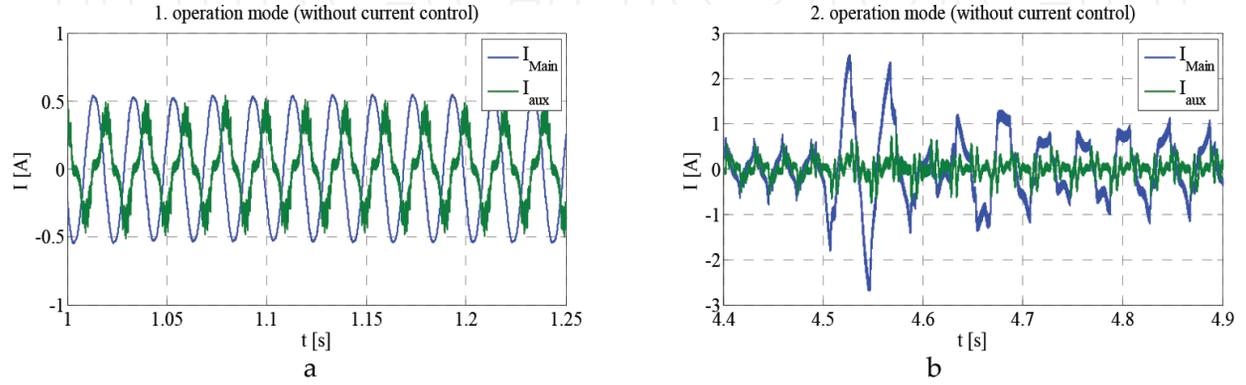

Figure 28. Stator currents of a single-phase induction motor fed by single-leg MxC; (a) in full-speed operation, and (b) reduced speed operation without LC filter and switched capacitor [17].

Currents are also highly deformed in both full-speed and reduced-speed regimes. In 4.5 seconds, it has changed the operation mode from full speed into reduced speed; speed of motor is proportional to the frequency of stator voltage of 25 Hz. Moreover, the start-up of the IM is not being successful. So, the main problem of single-leg matrix converter is high distortion of auxiliary-phase voltage and currents.

The basic principle of used current controlled PWM feedback loop is given in **Figure 29**.

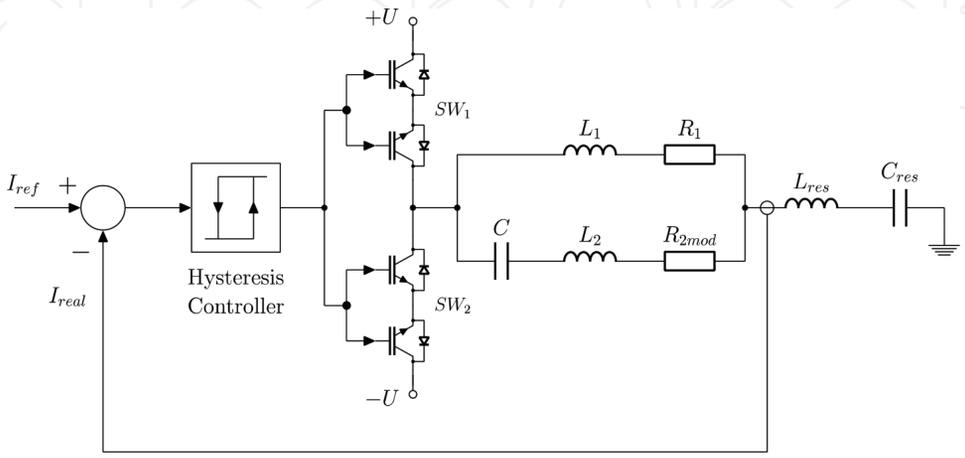

Figure 29. Principle of used CC-PWM feedback loop of single-leg MxC.

The resonant parts, L_{res}, C_{res}, have not been used at simulation of basic single-leg MxC in **Figure 28**.

5.3. Current control of single-phase induction motor fed by single-leg MxC using switched capacitor, LC filter and PWM control

Finally, combined solution with LC additional circuits and the current controlled PWM (hysteresis CC PWM) with current feedback closed loop is the best one. As mentioned in Section 4.2, simulation results of SLMxC with switched capacitors and LC filter under motoric IM load with PWM control are shown in figures in Section 6. There are shown steady-state currents and voltages of main and auxiliary phases in **Figure 25** at 33.33 Hz

Using this solution, the total harmonic distortion of main- and auxiliary-phase currents will be smaller than usually requested value of 5%.

Except the phase angle control, the amplitude of the phase currents must be controlled to optimal FOC operation of the induction machine under different load conditions.

6. Reached simulation results and discussion

All simulations of SLMxC with RL load were worked out in LT Spice environment. All simulations of SLMxC with motoric IM load were done in Matlab/Simulink programming environment.

Main- and auxiliary-phase steady-state currents and SLLC MxC output voltages have been worked-out at different frequencies 50/33.33/25/10 Hz.

The simulated phase currents under the RL load show that by control of switched capacitor the exact value of demanded capacitance is reached. Then, the phase angle between the mentioned current is also equal 90° as in **Figure 17**. From the **Figures 22–25**, it is obvious that this condition is satisfied.

Simulation of steady-state and start-up operation of two-phase IM is given in **Figures 24–26**. The simulation was done both with switched capacitor and LC resonant filter (except 50 Hz). Parameters are used for simulation with the induction machine:

$f = 50$ Hz; $U_{\text{rms}} = 230$ V; $P_{\text{av}} = 150$ W; $R_{\text{main}} = 58,85\ \Omega$; $R_{\text{aux}} = 66,1\ \Omega$; $L_{\text{main}} = 95$ mH; $L_{\text{aux}} = 120$ mH; M= 250 mH, $C_{50} = 20$ μF; $L_{\text{res}} = 274$ mH, $C_{\text{res}} = 37$ μF; and $q = 1$.

The simulated phase currents of the two-phase induction machine show that by control of switched capacitor reaches exact value of capacitance which in case of that the phase angle between the mentioned current is also equal 90°. The effect of the filter in a common phase will result in nearly the same magnitude of the IM currents during start-up; however, the time during start-up is rather longer.

7. Conclusion

The chapter brings analysis, modeling, and computer simulation of two-phase inverters focused on minimum switching devices. There are described two main types of switching devices: the single-leg VSI inverter partially known from a literature and single-leg MxC matrix converter as a new one. Since one-leg matrix converter type features a non-harmonic current waveform, the main emphasis is laid on the enhancement to their shapes. Because the use of classical PWM technique is restricted by insufficiency of voltage under basic frequency operation, it is necessary to use an additional hardware LC resonant circuit. After realization of above measures with LC filter, the total harmonic distortion of main- and auxiliary-phase currents will be much better: about 12% at 50 Hz and circa 9% at 33.33 Hz with LC circuits, see **Figure 24** in the text. By suitable design of LC elements, it is possible to reach the best value of the main- and auxiliary-phase current THDs (<5%) but the size of the LC elements will be high. Using that solution the total harmonic distortion of main- and auxiliary-phase currents will be smaller than usually requested value 5%. Analysis and worked-out simulation experiment results under RL load have shown that use of the LC filter can significantly improve the harmonic of the current waveform in both main- and auxiliary-phase windings. It should be also noticed that the simple LC resonant tank is always tuned to single frequency only and therefore the right operation of the MxC converter is also limited to this one frequency. To eliminate this disadvantage, the switched capacitor is supposed to use the capacitance that can be continuously changed and adapted to actual requirement given by an operational frequency. It is very important under field-oriented control of split-single-phase induction motor as a load for the converter. The basic topology has been completed by the LC filters that have both currents of main and auxiliary phases approximately sinusoidal waveforms. Main contribution of the paper is combined with the control of auxiliary phase advancing to be 90 degree under entire range of load operation and also pulse-width-modulation for field-oriented control.

Simulation experiments have been done using passive RL load and also split-winding single-phase IM motor. Worked-out results under RL load operation have shown very good

agreement with theoretical assumptions. Worked-out results under split-winding single-phase IM motoring operation are just preliminary ones because it needs accurate real motor parameters and takes longer time. Cooperation of switched capacitor single-leg LC matrix converter with split-winding single-phase IM is intended as for next work. The results reached can be served for usage and analysis of systems with two-phase ac motor drive. So, the next work is to focus on motoric load operation.

Acknowledgements

Results of this work were made with support of the Slovak Grant Agencies VEGA by the grant no. 1/0928/15 and APVV no. 0314/12. Authors also thank to the R&D operational program Centre of excellence of power electronics systems and materials for their components no. OPVaV-2008/01-SORO, ITMS 2622012003 funded by the European regional development fund (ERDF).

Nomenclature

LCL2C2	Center tapped series-parallel resonant LC filter
THD	Total harmonic distortion
VSI	Voltage source inverter
MxC	Matrix converter
PWM	Pulse-width-modulation
SVPWM	Space vector pulse-width-modulation
IM	Induction motor
DC	Direct current
MOSFET	Metal-oxide-semiconductor field-effect transistor
CC-PWM	Current controlled pulse-width-modulation
FOC	Field-oriented control
u_{aux}	Converter output voltage for auxiliary phase
u_{mxc}	Converter output voltage common for main and auxiliary phase
U_M	Voltage magnitude
f_{mxc}	Frequency of matrix converter output voltage
f_{ac}	Frequency of matrix converter input voltage
T_{mxc}	Period of matrix converter output voltage
T_{ac}	Period of matrix converter input voltage
Z_{main}	Impedance of main phase
Z_{aux}	Impedance of auxiliary phase
C_{aux}	Capacitance in auxiliary phase
C_{res}	Capacitance in resonant filter
L_{res}	Inductance in resonant filter

A_1	Fundamental harmonics amplitude
D_{tc}	Duty cycle
E	Energy
R_s	Resistance of IM stator winding
R_r	Resistance of IM rotor winding
L_s	Inductance of IM stator winding
L_r	Inductance of IM rotor winding
L_m	Mutual inductance
T_e	Electromagnetic torque
ω_m	Mechanical angular speed
pp	Number of pole pairs
N	Ratio between the effective numbers of turns in the auxiliary and the main stator windings

Author details

Branislav Dobrucky[1]*, Tomas Laskody[2] and Roman Konarik[1]

*Address all correspondence to: branislav.dobrucky@fel.uniza.sk

1 Department of Mechatronics and Electronics, Faculty of Electrical Engineering, University of Zilina, Zilina, Slovak Republic

2 BSH Drives and Pumps s.r.o., Michalovce, Slovak Republic

References

[1] Blalock T. J.: The first poly-phase system—a look back at two-phase power for AC distribution, IEEE Power and Energy Magazine, March-April 2004, p. 63, ISSN 1540-7977.

[2] Blaabjerg F., Lungeanu F., Skaug K., Tonnes M.: Two-phase induction motor drives, IEEE Transactions on Industry Applications, vol. 10, no. 4, July/August 2004, pp. 24–32.

[3] Blaabjerg F.: Evaluation of low-cost topologies for two-phase im drives in industrial application, Record of 37th IEEE IAS Annual Meeting on Industry Application, vol. 4, 2001, pp. 2358–2365, ISSN 0197-2618.

[4] Kinnares V., Charumit C.: Modulating functions of space vector PWM for three-leg VSI-fed unbalanced two-phase induction motors, IEEE Transactions on Power Electronics, vol. 24, no. 4, April 2009, pp. 1135–1139.

[5] Mhango L. M. C., Perryman R.: Analysis and simulation of a high-speed two-phase AC drive for aerospace applications, Electric Power Applications, IEE Proceedings, vol. 144, no.2, March 1997, pp. 149–157.

[6] Jang Do-Hyun.: PWM methods for two-phase inverters, IEEE Industry Applications Magazine, vol. 13, no. 2, March/April 2007, pp. 50–56.

[7] Klíma J.: Analytical model of induction motor fed from four-switch space vector PWM inverter. Time domain analysis, Acta Technica CSAV", vol. 44, 1999, pp. 393–410.

[8] Vodovozov V., Lillo N., Raud Z.: Single-phase electric drive for automotive applications, in Proc. of Int'l Symposium on Power Electronics, Electrical Drives, Automation and Motion SPEEDAM'14, Ischia, 2014, pp. 1293–1298.

[9] Schreier L., Chomat M., Klima J.: Analysis of three-phase induction machine operation under two-phase supply. In Proc. of the IEEE-ICIT 02 Conf., Bangkok (Thailand), 2002, ISBN 0-7803-7657-9, pp. 107–112.

[10] Chomat M., Lipo T.: Adjustable-speed single-phase IM drive with reduced number of switches, IEEE Transactions on Industry Applications, vol. 39, no. 3, May/June 2003, pp. 819–825.

[11] Chomat M., Lipo T. A.: Adjustable-speed drive with single-phase induction machine for HVAC applications, in Proc. IEEE PESC'01, 2001, pp. 1446–1451.

[12] Chomat M., Lipo T. A.: Adjustable-Speed single-phase IM drive with reduced number of switches, in Conf. Rec. IEEE-IAS Annu. Meeting, 2001, pp. 1800–1806.

[13] Lettenmainer A., Novotny D., Lipo T. A.: Single-phase induction motor with an electronically controlled capacitor, IEEE Transactions Industry Applications, vol. 27, no. 1, 1988, pp. 38–43.

[14] Danila A., Margineanu I., Campeanu R., Suciu C., Boian I.: The optimization of the single-two phase induction motor start-up with electronically switched capacitor, in Proc. of IEEE Int'l Conf. on Automation, Quality and Testing, Robotics, (AQTR 2008), Cluj-Napoca, vol. 3, 2008, pp. 450–453.

[15] Kaščák S., Laškody T., Praženica M., Koňarik R.: Current control contribution to a single-phase induction motor fed by single-leg voltage source inverter, Proc. of IEEE Int'l Conf. ELEKTRO, Zilina, 2016, DOI: 10.1109/ELEKTRO.2016.7512059.

[16] Laškody T., Dobrucký B, Kascak S, Praženica M.: 2-phase direct torque controlled IM drive using SVPWM with torque ripple reduction: Motoring and regenerating, Industrial Electronics (ISIE), 2014 IEEE 23rd International Symposium on, 1–4 June 2014, pp. 698–702.

[17] Dobrucký B., Laškody T., Praženica M.: A novel supply system for two-phase induction motor by single leg matrix converter. Elektronika ir Elektrotechnika, vol. 21, no. 4, 2015, ISSN 1392-1215, pp. 13–16.

[18] Zuckerberger A., Weinstock D., Alexandrovitz A.: Single-phase matrix converter, IEE Proc. Electric Power Appl., vol. 144, no. 4, Jul 1997, pp. 235–240.

[19] Koňarik R., Dobrucký B., Štefanec P.: Improved two-phase one-leg matrix converter using L-C filter. In Proc. of MEIT 2016 Int'l Conf. on Mechanical, Electronic and Information Technology, August 28–29, 2016, Phuket, Thailand, pp. TBA.

[20] Dobrucký B., Beňová M., Abdalmula M., Kaščák S.: Design analysis of LCTLC resonant inverter for two-stage 2-phase supply system, Automatika, vol. 54, no. 3, 2014, pp. 299–307, ISSN 0005-11-44.

[21] Laškody T.: Progressive control methods of two-phase motors, Ph.D. Thesis, Reg. No. 28260020163453, Faculty of Electrical Engineering, University of Zilina, August 2016.

[22] Dobrucký B., Praženica M., Kassa J.: Topology and control strategies for two-phase electronic converter drives, International Symposium on Power Electronics, Electrical Drives, Automation and Motion, SPEEDAM 2010, Pisa, pp. 1319–1324.